2018-11

Numerical Solution of a Nonlinear Diffusion Model with Memory

Thornton, Grant D.; Anderson, Benjamin R.; Baugh, Matthew A.; Robertson, Grant M.; Shapiro, Jessica; Thyberg, Robert C.; Neta, Beny

Monterey, California. Naval Postgraduate School

NPS-MA-18-001

NAVAL POSTGRADUATE SCHOOL

MONTEREY, CALIFORNIA

NUMERICAL SOLUTION OF A NONLINEAR DIFFUSION MODEL WITH MEMORY

by

Grant D. Thornton, Benjamin R. Anderson, Matthew A. Baugh, Grant M. Robertson, Jessica Shapiro, Robert C. Thyberg, Beny Neta

November 2018

Approved for public release; distribution is unlimited

Prepared for: Naval Postgraduate School

THIS PAGE INTENTIONALLY LEFT BLANK

REPORT DOCUMENTATION PAGE

Form Approved
OMB No. 0704-0188

1. REPORT DATE *(DD-MM-YYYY)*	**2. REPORT TYPE**	**3. DATES COVERED** *(From-To)*
26-09-2018	Technical Report	07-01-2018 - 09-30-2018

4. TITLE AND SUBTITLE
Numerical Solution of a Nonlinear Diffusion Model with Memory

5a. CONTRACT NUMBER

5b. GRANT NUMBER

5c. PROGRAM ELEMENT NUMBER

6. AUTHOR(S)
Grant Thornton, Benjamin Anderson, Matthew Baugh, Grant Robertson, Jessica Shapiro, Robert Thyberg, Beny Neta

5d. PROJECT NUMBER

5e. TASK NUMBER

5f. WORK UNIT NUMBER

7. PERFORMING ORGANIZATION NAME(S) AND ADDRESS(ES) AND ADDRESS(ES)
Naval Postgraduate School

8. PERFORMING ORGANIZATION REPORT NUMBER
NPS-MA-18-001

9. SPONSORING / MONITORING AGENCY NAME(S) AND ADDRESS(ES)

10. SPONSOR/MONITOR'S ACRONYM(S)

11. SPONSOR/MONITOR'S REPORT NUMBER(S)

12. DISTRIBUTION / AVAILABILITY STATEMENT
Approved for public release; distribution is unlimited

13. SUPPLEMENTARY NOTES

14. ABSTRACT

Finite difference approximation of a nonlinear integro-differential equation associated with the penetration of a magnetic field into a substance is studied. Here we discuss the model described by a nonlinear integro-differential equation. The system of time dependent ordinary differential equations is solved using Runge-Kutta method with adaptive step size. The time integral make this a non-trivial application of the Matlab code ODE45. Eight examples are given with mostly homogeneous boundary conditions. The results show that when the analytic solution is not growing in time, then the solution decays at a rate proven theoretically in the literature.

15. SUBJECT TERMS
Nonlinear integro-differential equations, large time behavior, finite difference scheme.

16. SECURITY CLASSIFICATION OF:			**17. LIMITATION OF ABSTRACT**	**18. NUMBER OF PAGES**	**19a. NAME OF RESPONSIBLE PERSON**
a. REPORT	**b. ABSTRACT**	**c. THIS PAGE**			Beny Neta
Unclassified	Unclassified	Unclassified	UU	28	**19b. TELEPHONE NUMBER** *(include area code)* 831 656 2235

THIS PAGE INTENTIONALLY LEFT BLANK

NAVAL POSTGRADUATE SCHOOL
Monterey, California 93943-5000

Ronald A. Route
President

Steven Lerman
Provost

The report entitled "Numerical Solution of a Nonlinear Diffusion Model with Memory" was prepared for and funded by Naval Postgraduate School.

Further distribution of all or part of this report is authorized.

This report was prepared by:

Grant Thornton
ENS, USN

Benjamin Anderson
ENS, USN

Matthew Baugh
ENS, USN

Grant Robertson
ENS, USN

Jessica Shapiro
LT, USN

Robert Thyberg
ENS, USN

Beny Neta
Professor
Department of Applied Mathematics

Reviewed by:

Wei Kang, Chairman
Department of Applied Mathematics

Released by:

Jeffrey D. Paduan
Dean of Research

THIS PAGE INTENTIONALLY LEFT BLANK

Numerical solution of a nonlinear diffusion model with memory

ENS Grant D. Thornton, USN
ENS Benjamin R. Anderson, USN
ENS Matthew A. Baugh, USN
ENS Grant M. Robertson, USN
LT Jessica Shapiro, USN
ENS Robert C. Thyberg, USN
and
Professor Beny Neta
Department of Applied Mathematics
Naval Postgraduate School
Monterey, CA 93943
U. S. A.

October 3, 2018

Abstract. Finite difference approximation of a nonlinear integro-differential equation associated with the penetration of a magnetic field into a substance is studied. Here we discuss the model described by a nonlinear integro-differential equation. The system of time dependent ordinary differential equations is solved using Runge-Kutta method with adaptive step size. The time integral make this a non-trivial application of the Matlab code ODE45. Eight examples are given with mostly homogeneous boundary conditions. The results show that when the analytic solution is not growing in time, then the solution decays at a rate proven theoretically in the literature.

Key words and phrases: Nonlinear integro-differential equations, large time behavior, finite difference scheme.

AMS subject classification: 45K05, 65N06, 35K55.

1 Introduction

Integro-differential equations and systems of such equations arise in the study of various problems in physics, chemistry, technology, economics etc. See [1] for more details and theoretical results. Such systems arise, for instance, for mathematical modelling of the process of penetrating of magnetic field in the substance. If the coefficient of thermal heat capacity and electroconductivity of the substance highly dependent on temperature, then the Maxwell's system, that describe the process of penetration of a magnetic field into a substance [2], can be rewritten in the following form [3]:

$$\frac{\partial H}{\partial t} = -rot\left[a\left(\int_0^t |rotH|^2\, d\tau\right) rotH\right], \tag{1.1}$$

where $H = (H_1, H_2, H_3)$ is a vector of the magnetic field and the function $a = a(S)$ is defined for $S \in [0, \infty)$.

If the magnetic field has the form $H = (0, 0, U)$ and $U = U(x, t)$, then we have

$$rot(a(S)rotH) = \left(0,\ 0,\ -\frac{\partial}{\partial x}\left(a(S)\frac{\partial U}{\partial x}\right)\right).$$

Therefore, we obtain the following nonlinear integro-differential equation:

$$\frac{\partial U}{\partial t} = \frac{\partial}{\partial x}\left[a\left(\int_0^t \left[\left(\frac{\partial U}{\partial x}\right)^2\right] d\tau\right)\frac{\partial U}{\partial x}\right], \tag{1.2}$$

Note that (1.2) is complex, but special cases were investigated, see [3]-[8]. The existence of global solutions for initial-boundary value problems of such models have been proven in [3],[4],[8] by using the Galerkin and compactness methods [9],[10]. For solvability and uniqueness properties for initial-boundary value problems (1.2), see e.g. [5]-[7]. The asymptotic behavior of the solutions of (1.2) have been the subject of intensive research in recent years, (see e.g. [1], [8],[11]).

Laptev [6] proposed some generalization of equations of type (1.1). Assume the temperature of the considered body is constant throughout the material, i.e., depending on time, but independent of the space coordinates. If the magnetic field again has the form $H = (0, 0, U)$ and $U = U(x, t)$, then the same process of penetration of the magnetic field into the material is modeled by the following

integro-differential equation [6]:

$$\frac{\partial U}{\partial t} = a\left(\int_0^t \int_0^1 \left[\left(\frac{\partial U}{\partial x}\right)^2\right] dx d\tau\right) \frac{\partial^2 U}{\partial x^2}. \tag{1.3}$$

The purpose of this work is to study the finite difference approximation for the case $a(S) = 1+S$. The solvability, uniqueness and asymptotics to the solutions of (1.3) type scalar models are studied in [8] and [12].

Note that in [13] and [14] difference schemes for (1.2) type models were investigated. Difference schemes for one nonlinear parabolic integro-differential scalar model similar to (1.2) were studied in [15]. Difference schemes for the scalar equation of (1.3) type with $a(S) = 1 + S$ were studied in [16].

The rest of this report is organized as follows. In the second section the finite difference scheme for (1.3) is investigated. In the third section we present several numerical examples with homogeneous and non-homogeneous boundary conditions. These results validate the theoretical results found in the literature.

2 Finite difference scheme

In the rectangle $Q_T = (0,1) \times (0,T)$, where T is a positive constant, we discuss finite difference approximation of the nonlinear integro-differential problem:

$$\frac{\partial U}{\partial t} - \left\{1 + \int_0^t \int_0^1 \left[\left(\frac{\partial U}{\partial x}\right)^2\right] dx d\tau\right\} \frac{\partial^2 U}{\partial x^2} = f(x,t), \tag{2.1}$$

$$U(0,t) = U(1,t) = 0, \tag{2.2}$$

$$U(x,0) = U_0(x). \tag{2.3}$$

Here $f_1 = f(x,t)$, $U_0 = U_0(x)$ are given sufficiently smooth functions of their arguments.

We introduce a net in the rectangle Q_T whose mesh points are denoted by $(x_i, t_j) = (ih, j\tau)$, where $i = 0, 1, ..., M$ and $j = 0, 1, ..., N$ with $h = 1/M$, $\tau = T/N$. The initial line is denoted by $j = 0$. The discrete approximation at (x_i, t_j) is denoted by u_i^j, v_i^j and the exact solution to the problem (2.1)-(2.3) at those points by U_i^j. We will use the following notations for the differences and norms:

$$\Delta_x r_i^j = \frac{r_{i+1}^j - r_i^j}{h}, \quad \nabla_x r_i^j = \frac{r_i^j - r_{i-1}^j}{h},$$

$$\|r\|_h = \left(\sum_{i=1}^{M-1} r_i^2 h\right)^{1/2}, \quad \|r]|_h = \left(\sum_{i=1}^{M} r_i^2 h\right)^{1/2}.$$

Thus we have

$$\begin{gathered} \frac{du}{dt}|_i^j - \{1 + S_j\} \Delta_x \nabla_x u_i^{j+1} = f_i^j, \\ i = 1, 2, ..., M-1; \;\; j = 0, 1, ..., N-1, \end{gathered} \tag{2.4}$$

$$u_0^j = u_M^j = 0, \quad j = 0, 1, ..., N, \tag{2.5}$$

$$u_i^0 = U_{0,i}, \quad i = 0, 1, ..., M, \tag{2.6}$$

where

$$S_j = \tau h \sum_{l=1}^{M} (\nabla_x u_l^j)^2 + S_{j-1} \tag{2.7}$$

and $S_0 = 0$.

The system of ODEs (2.4) will be solved using Runge-Kutta-Fehlberg of orders four and five, see [18], (Matlab routine ODE45) using adaptive time step. Because of the integral over time on the right, we had to call ODE45 for each time sub-interval of length τ to be chosen by the user. The relative error tolerance set to 10^{-6} and the relative error tolerance is set to 10^{-3}.

Jangveladze et al. [1] have shown that

$$\|u^n\|_h^2 + \sum_{j=1}^{n} \|\nabla_x u^j]|_h^2 \tau < C, \quad n = 1, 2, ..., N. \tag{2.8}$$

In (2.8) the constant C depends on T and on f respectively.

The a-priori estimate (2.8) guarantees the stability and existence, see [10], of solution of the scheme (2.4)-(2.6).

Remark: Note, that according to the scheme of proving convergence theorem, the uniqueness of the solution of the scheme (2.4)-(2.6) can be proven. In particular, assuming the existence of two solutions u and $\bar{u}$ of the scheme (2.4)-(2.6), then for the differences $\bar{y} = u - \bar{u}$ we get $\|\bar{y}^n\|_h^2 \leq 0, \quad n = 1, 2, ..., N$. So, $\bar{y} \equiv 0$.

3 Numerical results

In this section, we list eight examples for which we choose $f(x,t)$ so that the exact solution is given. All examples but the last are problems with homogeneous boundary conditions. Most of the examples have a solution decaying in time. We will plot the numerical and anlytic solutions side by side as well as plotting the difference between the two as a function of x and t. We also demonstarte how the error changes when we refine the spatial grid for a fixed time step and similarly when we fix the spatial grid and reduce the time step.

Example 1:

In our first numerical experiment we have chosen the right hand side so that the exact solution is given by

$$U(x,t) = e^{-t} \sin(\pi x).$$

In this case the right hand side is

$$f(x,t) = e^{-t} sin(\pi x)(-1 + \pi^2 + \pi^4/4(1 - e^{-2t}))$$

The numerical solution is plotted in Figure 1 using $M = 100$ grid points and to its right the analytic solution. We also plotted the absolute error in Figure 2 and the RMS error as a function of t in Figure 3. The RMS error is given by

$$uerr(t) = \sqrt{\sum_{i=1}^{M} (u(i,t) - U(i,t))^2} \tag{3.1}$$

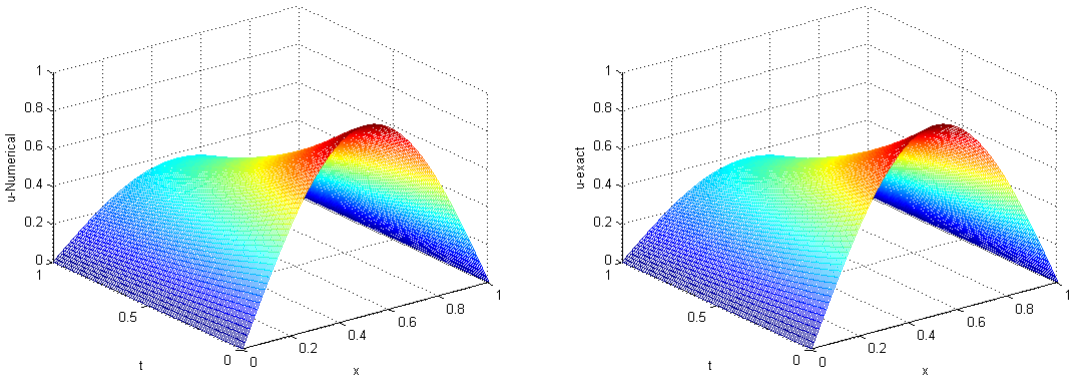

Figure 1: The numerical solution (left) and the analytic solution (right) for the first example

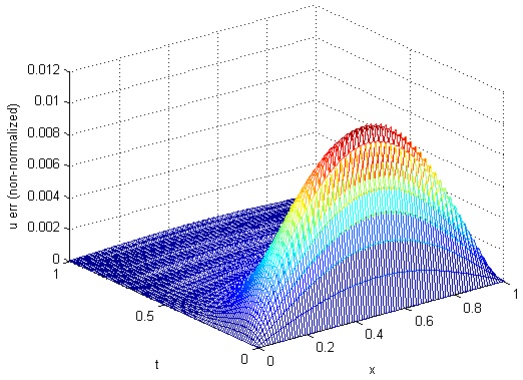

Figure 2: The absolute error between the numerical solution and the analytic solution for the first example

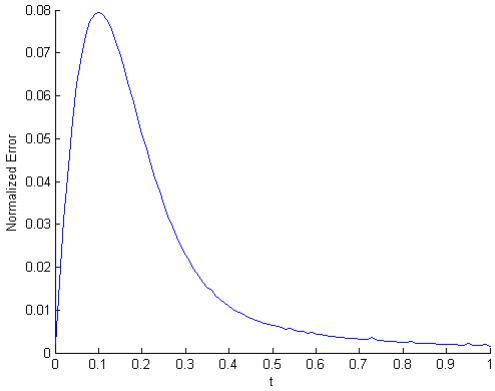

Figure 3: The RMS error as a function of t for the first example

We also give the RMS error as a function of t for various values of grid spacing, i.e. $M = 4, 8, 16, 32, 64$ for a fixed time step and the same error for a fixed M and various values of time steps $\tau = 0.25, 0.125, 0.0625, 0.03125, 0.015625$ in Figure 4.

It can be seen that the error increases initially for all M but eventually goes to zero. The rate of decay increases with increasing M. Similar situation can be seen when M is fixed and the time step is halved.

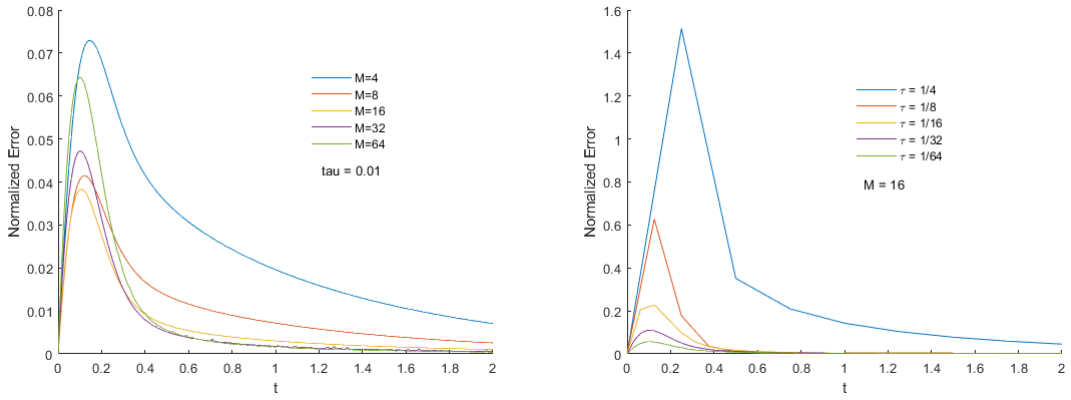

Figure 4: The RMS error as a function of t for fixed time step $\tau = 0.01$ and increasing M (left) and for fixed $M = 16$ and halving the time step (right) for the first example

Example 2:

$$U(x,t) = \cos(2\pi t)\sin(\pi x).$$

In this case the right hand side is

$$f(x,t) = -2\pi\sin(2\pi t)\sin(\pi x) + \pi^2\left(1 - \pi^2\cos(2\pi t)\sin(\pi x)\right)\cos(2\pi t)\sin(\pi x).$$

The numerical solution is plotted in Figure 5 using $M = 100$ grid points and to its right the analytic solution. We also plotted the absolute error in Figure 6 and the RMS error (3.1) as a function of t in Figure 7.

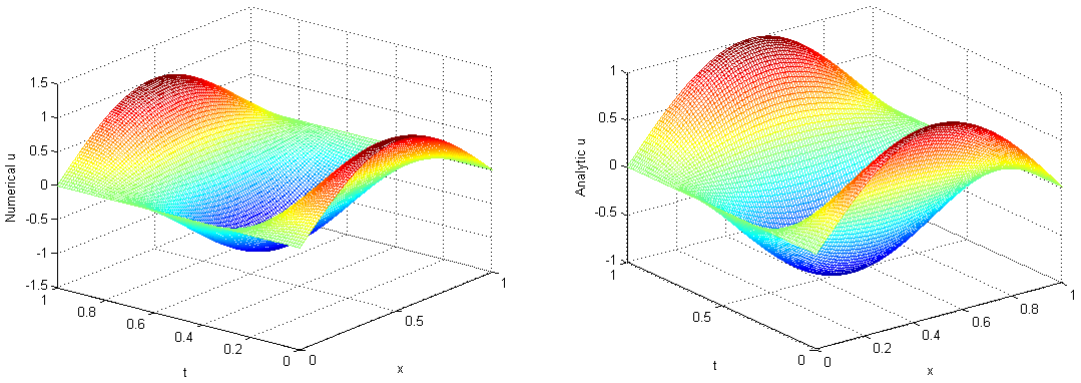

Figure 5: The numerical solution (left) and the analytic solution (right) for the second example

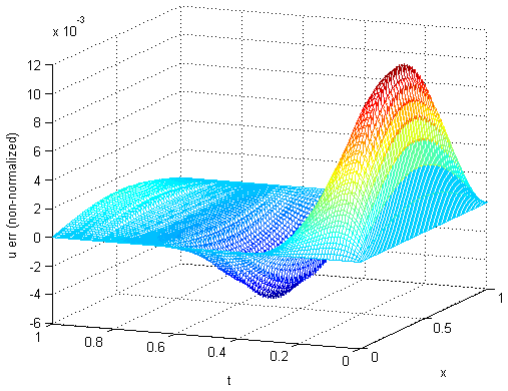

Figure 6: The absolute error between the numerical solution and the analytic solution for the second example

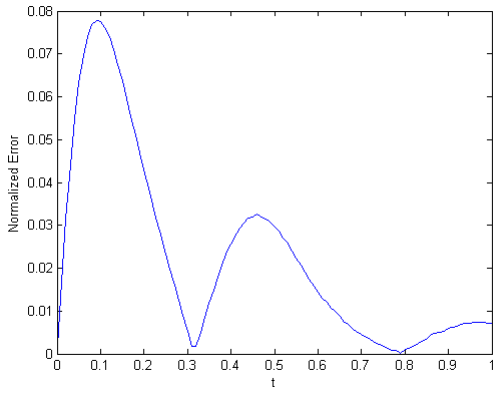

Figure 7: The RMS error as a function of t for the second example

We also give the RMS error as a function of t for various values of grid spacing, i.e. $M = 4, 8, 16, 32, 64$ for a fixed time step $\tau = 0.01$ and the same error for a fixed $M = 16$ and various values of time steps $\tau = 0.25, 0.125, 0.0625, 0.03125, 0.015625$ in Figure 8.

It can be seen that the error increases initially for all M but oscillating with diminishing amplitude. The rate of decay increases with increasing M. Similar situation can be seen when M is fixed and the time step is halved.

Example 3:

$$U(x,t) = x(x-1)(x+1)t.$$

In this case the right hand side is

$$f(x,t) = x(x-1)(x+1) - (1 + (4t^3/15)((2(x+1))t + (2(x-1))t + 2xt).$$

The numerical and analytic solutions are plotted in Figure 9 using $M = 100$ grid points and to its right the analytic solution. We also plotted the absolute error in Figure 10 and the RMS error (3.1) as a function of t in Figure 11.

We also give the RMS error as a function of t for various values of grid spacing, i.e. $M = 4, 8, 16, 32, 64$ for a fixed time step $\tau = 0.01$ and the same error for a fixed $M = 16$ and various values of time steps $\tau = 0.25, 0.125, 0.0625, 0.03125, 0.015625$ in Figure 12.

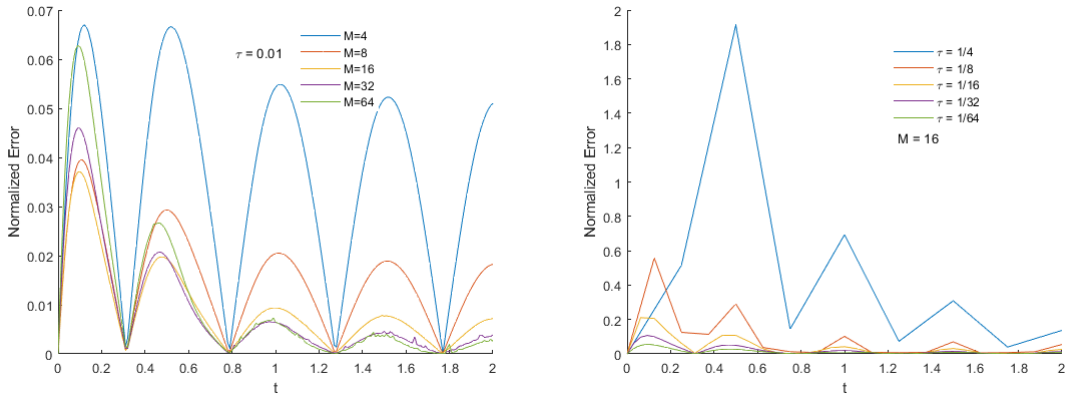

Figure 8: The RMS error as a function of t for fixed time step $\tau = 0.01$ and increasing M (left) and for fixed $M = 16$ and halving the time step (right) for the second example

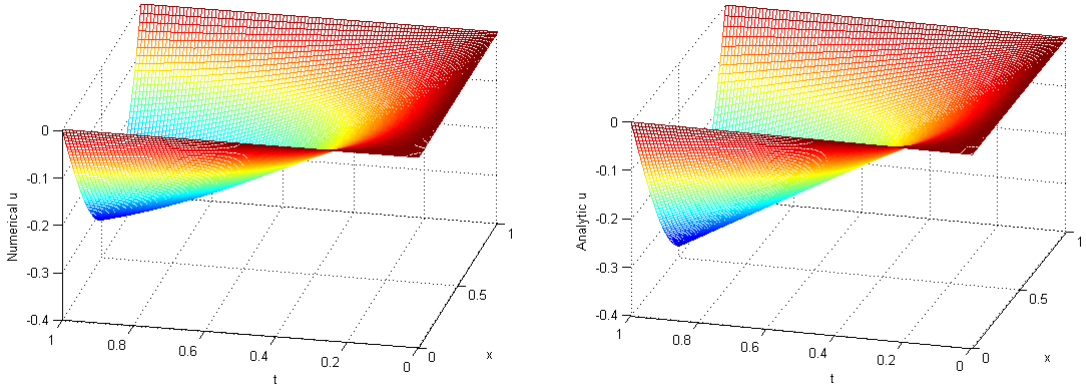

Figure 9: The numerical solution (left) and the analytic solution (right) for the third example

It can be seen that the error increases for all M since the solution is increasing as a function of t. Similar situation can be seen when M is fixed and the time step is halved.

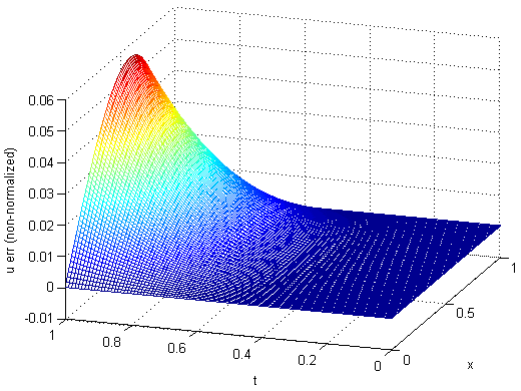

Figure 10: The absolute error between the numerical solution and the analytic solution for the third example

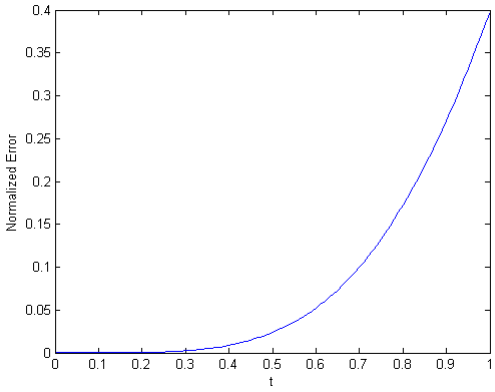

Figure 11: The RMS error as a function of t for the third example

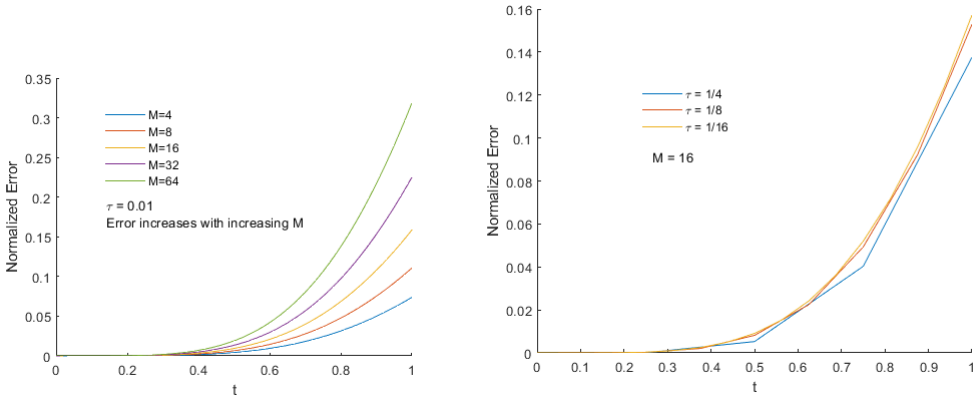

Figure 12: The RMS error as a function of t for a fixed time step $\tau = 0.01$ and increasing M (left) and for fixed $M = 16$ and halving the time step (right) for the third example

Example 4:

$$U(x,t) = e^{-t/2}\sin(3\pi x).$$

In this case the right hand side is

$$f(x,t) = -\frac{1}{2}e^{-t/2}\sin(3\pi x) + \left(9\pi^2\left(1 + \frac{9\pi^2}{2} - \frac{9\pi^2}{2}e^{-t}\right)\right)e^{-t/2}\sin(3\pi x).$$

The numerical solution is plotted in Figure 13 using $M = 100$ grid points and to its right and the analytic solution. We also plotted the absolute error in Figure 14 and the RMS error (3.1) as a function of t in Figure 15.

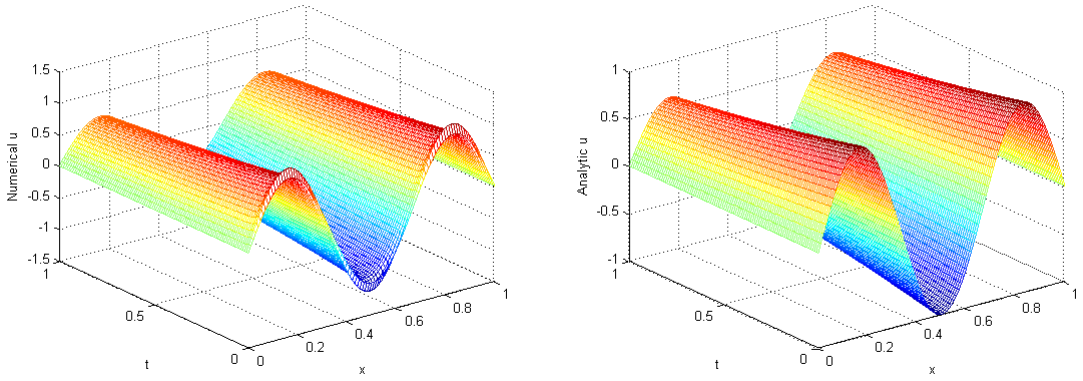

Figure 13: The numerical solution and the analytic solution for the fourth example using $M = 100$

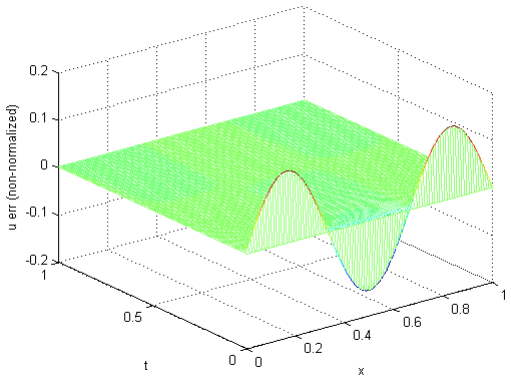

Figure 14: The absolute error between the numerical solution and the analytic solution for the fourth example

We also give the RMS error as a function of t for various values of grid spacing, i.e. $M = 4, 8, 16, 32, 64$ for a fixed time step $\tau = 0.01$ and the same error for a fixed $M = 16$ and various values of time steps $\tau = 0.25, 0.125, 0.0625, 0.03125, 0.015625$ in Figure 16.

It can be seen that the error increases initially for all M but eventually goes to zero. The rate of decay increases with increasing M. Similar situation can be seen when M is fixed and the time step is halved.

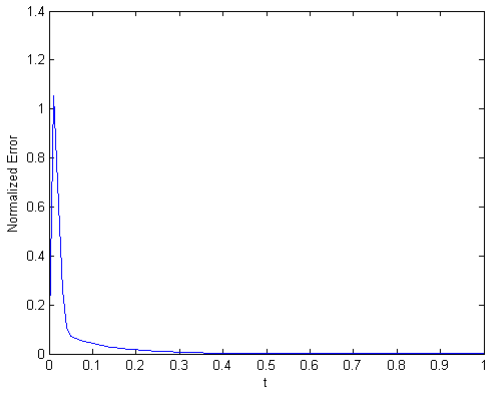

Figure 15: The RMS error as a function of t for the fourth example

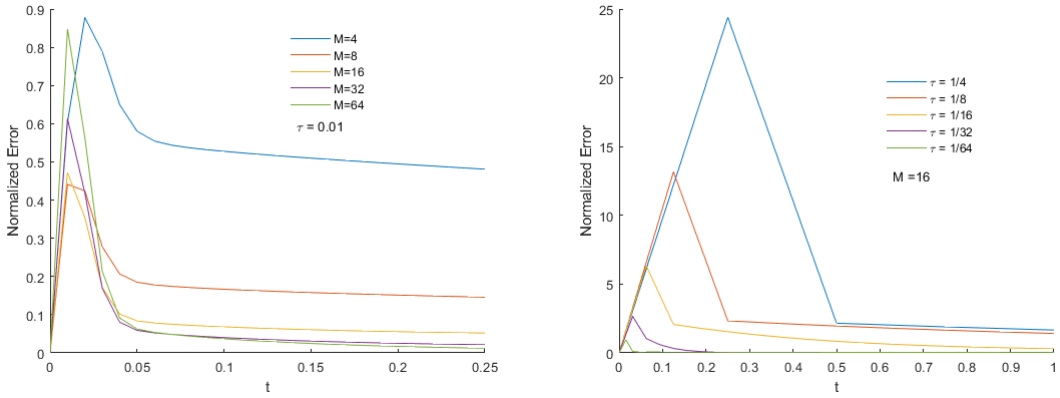

Figure 16: The RMS error as a function of t for fixed time step $\tau = 0.01$ and increasing M (left) and for fixed $M = 16$ and halving the time step for the fourth example

Example 5:

$$U(x,t) = (x^2 - x)(t^2 - t).$$

In this case the right hand side is

$$f(x,t) = x(x-1)(2t-1) - \left(1 + \frac{t^5}{15} - \frac{t^4}{6} + \frac{t^3}{9}\right)(2t^2 - 2t).$$

The numerical solution is plotted in Figure 17 using $M = 100$ grid points and to its right and the analytic solution. We also plotted the absolute error in Figure 18 and the RMS error (3.1) as a function of t in Figure 19.

We also give the RMS error as a function of t for various values of grid spacing, i.e. $M = 4, 8, 16, 32, 64$ for a fixed time step $\tau = 0.01$ and the same error for a fixed $M = 16$ and various values of time steps $\tau = 0.25, 0.125, 0.0625, 0.03125, 0.015625$ in Figure 20.

It can be seen that the error increases for all M since the solution increases as time increases.

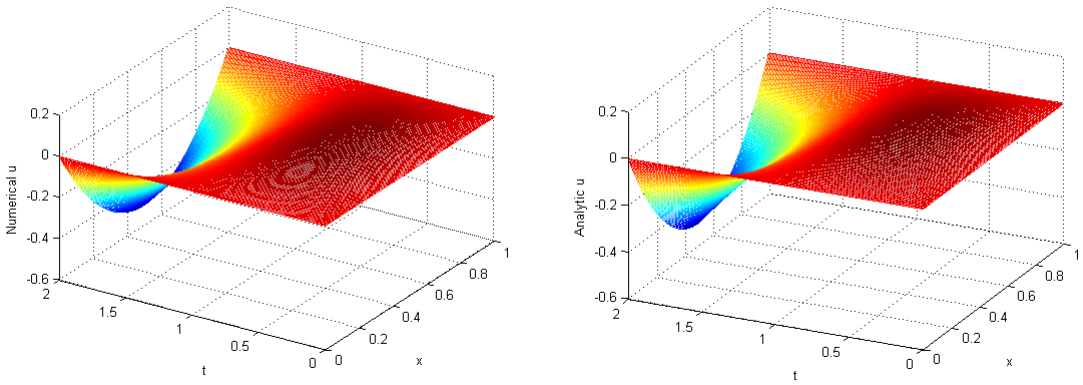

Figure 17: The numerical solution and the analytic solution for the fifth example

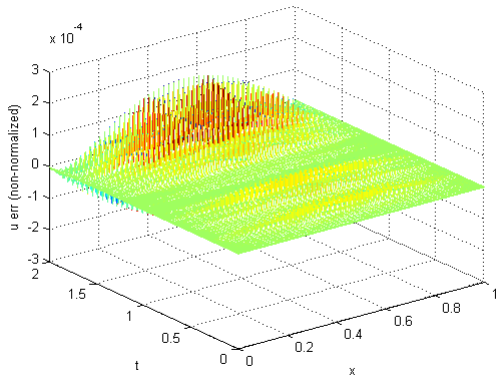

Figure 18: The absolute error between the numerical solution and the analytic solution for the fifth example

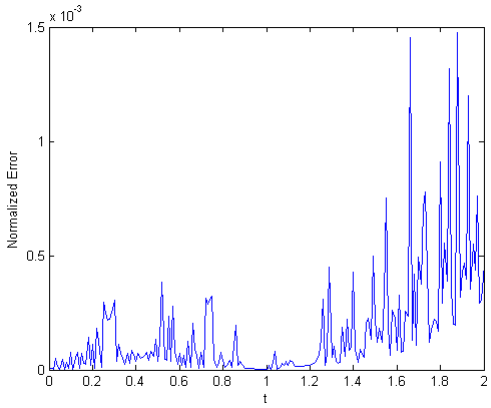

Figure 19: The RMS error as a function of t for the fifth example

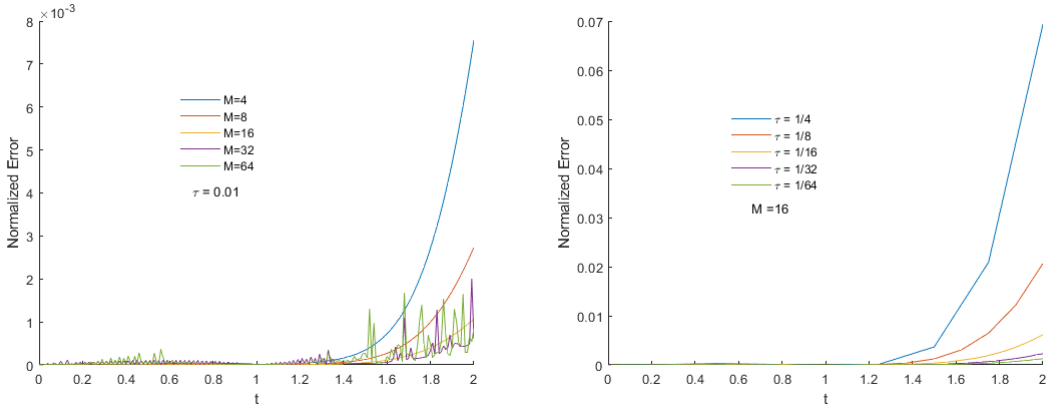

Figure 20: The RMS error as a function of t for fixed time step $\tau = 0.01$ and increasing M (left) and for fixed $M = 16$ and halving the time step for the fifth example

Example 6:

$$U(x,t) = x(1-x)e^{-2t}.$$

In this case the right hand side is

$$f(x,t) = -2x(x-1)e^{-2t} - \left(\frac{13 - e^{-4t}}{6}\right) e^{-2t}.$$

The numerical and analytic solutions ares plotted in Figure 21 using $M = 100$ grid points and to its right and the analytic solution. We also plotted the absolute error in Figure 22 and the RMS error (3.1) as a function of t in Figure 23.

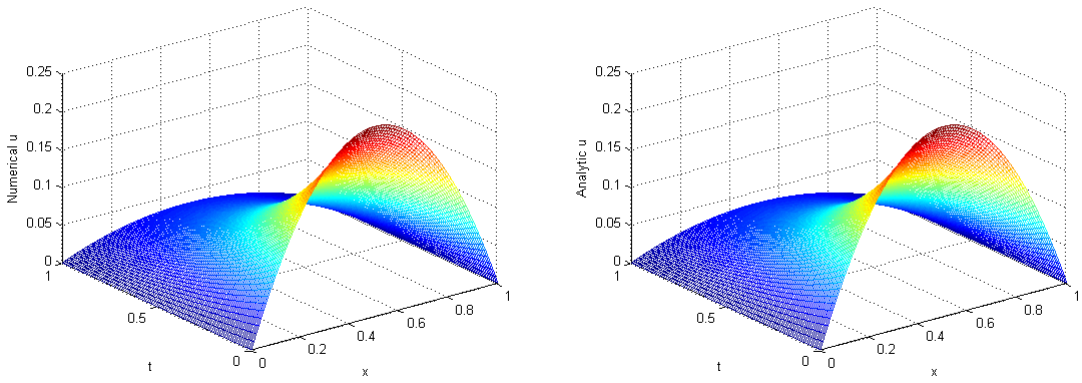

Figure 21: The numerical solution and the analytic solution for the sixth example.

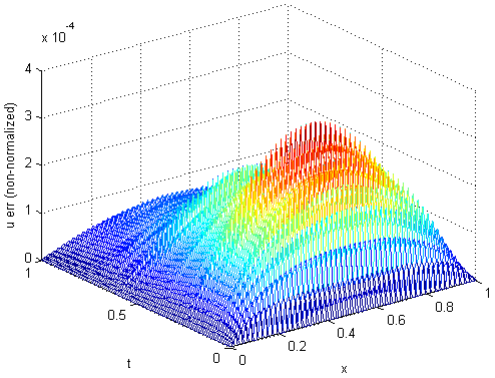

Figure 22: The absolute error between the numerical solution and the analytic solution for the sixth example

We also give the RMS error as a function of t for various values of grid spacing, i.e. $M = 4, 8, 16, 32, 64$ for a fixed time step and the same error for a fixed $M = 16$ and various values of time steps $\tau = 0.25, 0.125, 0.0625, 0.03125, 0.015625$ in Figure 24.

It can be seen that the error increases initially for all M but eventually goes to zero. The rate of decay increases with increasing M. Similar situation can be seen when M is fixed and the time step is halved.

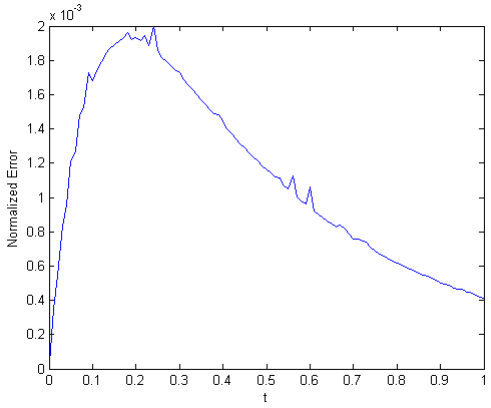

Figure 23: The RMS error as a function of t for the sixth example

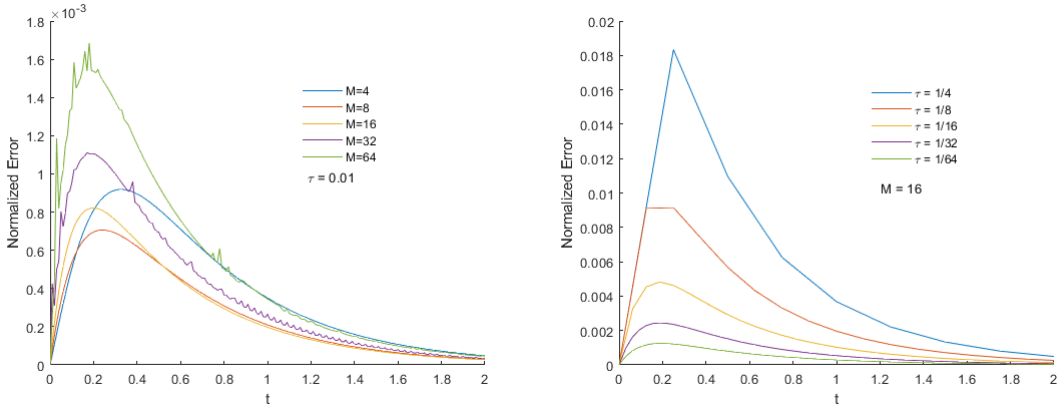

Figure 24: The RMS error as a function of t for fixed time step $\tau = 0.01$ and increasing M (left) and for fixed $M = 16$ and halving the time step for the sixth example

Example 7:

$$U(x,t) = x(1-x)\sin(x+t).$$

In this case the right hand side is

$$\begin{aligned} f(x,t) &= x(1-x)\cos(x+t) - (1+\tfrac{11}{60}t - \tfrac{1}{8}\sin(t)\cos(t) - \tfrac{1}{8}\sin(t)\cos(t+2)) \\ &\times \quad ((-2-x+x^2)\sin(x+t) + 2(1-2x)\cos(x+t)) \end{aligned}$$

The numerical solution is plotted in Figure 25 using $M = 100$ grid points and to its right and the analytic solution. We also plotted the absolute error in Figure 26 and the RMS error (3.1) as a function of t in Figure 27.

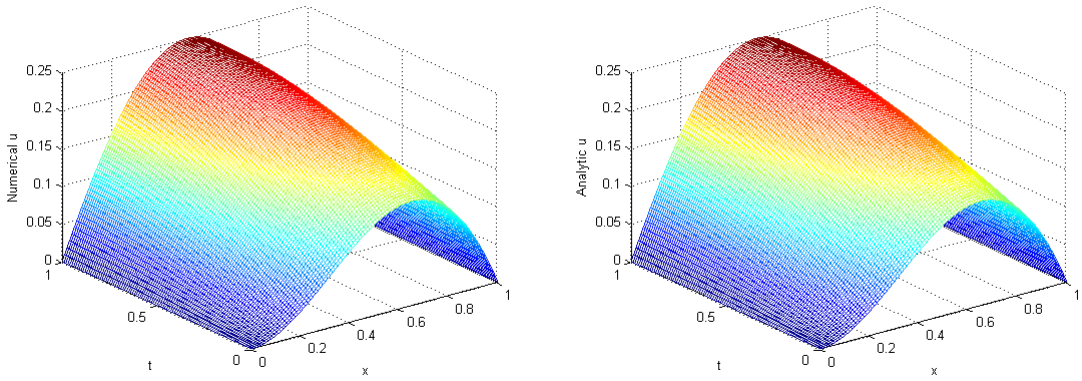

Figure 25: The numerical and the analytic solutions for the seventh example

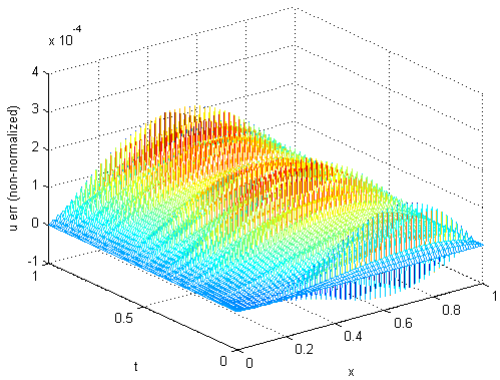

Figure 26: The absolute error between the numerical solution and the analytic solution for the seventh example

We also give the RMS error as a function of t for various values of grid spacing, i.e. $M = 4, 8, 16, 32, 64$ for a fixed time step and the same error for a fixed $M = 16$ and various values of time steps $\tau = 0.25, 0.125, 0.0625, 0.03125, 0.015625$ in Figure 28.

It can be seen that the error oscillates for all M with diminishing amplitude when decreasing τ or increasing M. The analytic solution is bounded for all t and the RMS error is also bounded.

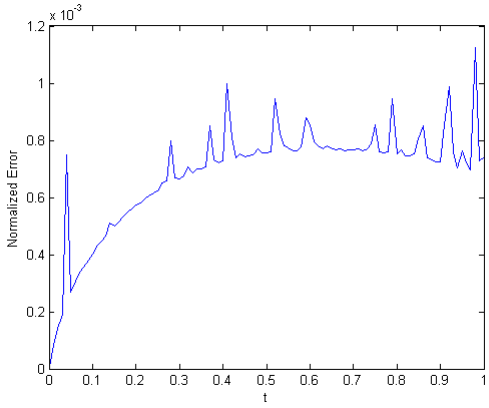

Figure 27: The RMS error as a function of t for the seventh example

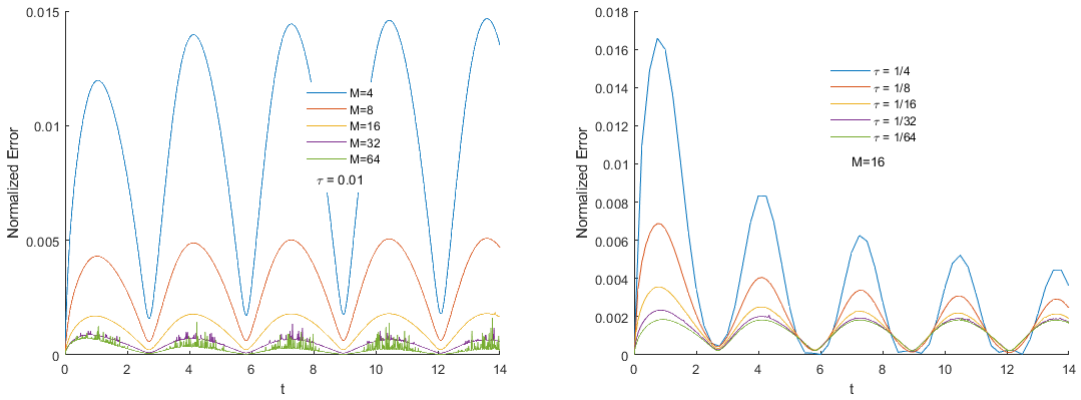

Figure 28: The RMS error as a function of t for fixed time step $\tau = 0.01$ and increasing M (left) and for fixed $M = 16$ and halving the time step for the seventh example

For this example, we also show that the analytic and numrical solutions (Figure 29) oscillate when t increases to $t = 5$.

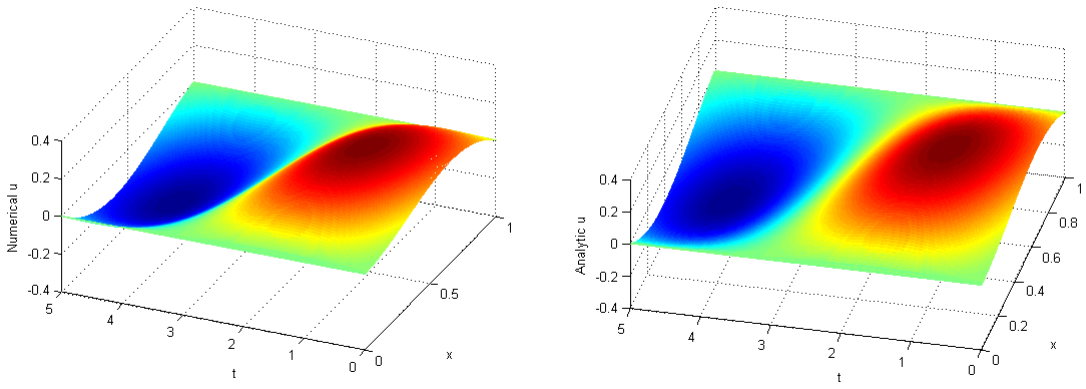

Figure 29: The numerical and the analytic solutions for the seventh example

Example 8:
In our last example, we have taken a non-homogeneous boundary conditions.

$$U(x,t) = x(x-1)t + x^2 + 1.$$

In this case the right hand side is

$$f(x,t) \quad = \quad x^2 - x - (1 + \tfrac{t^3}{9} + \tfrac{t^2}{3} + \tfrac{4t}{3})(2t+2)$$

The boundary conditions are

$$u(0,t) = 1,$$
$$u(1,t) = 2.$$

The numerical solution is plotted in Figure 30 using $M = 100$ grid points and to its right and the analytic solution. We also plotted the absolute error in Figure 31 and the RMS error (3.1) as a function of t in Figure 32.

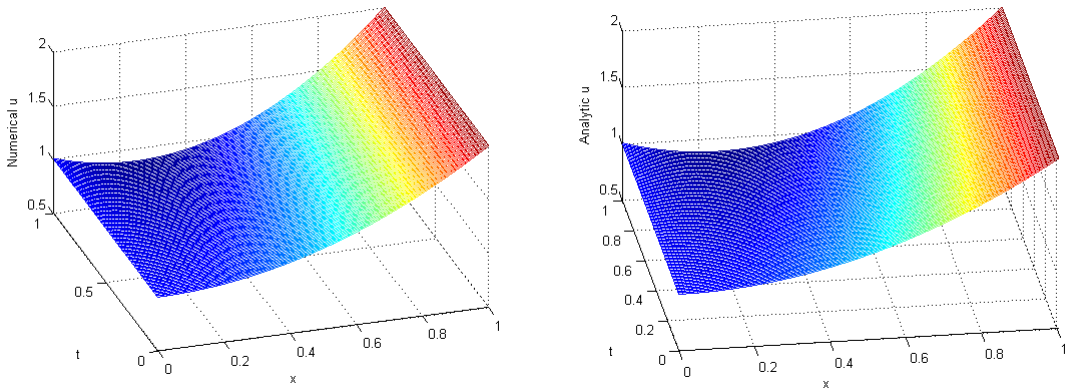

Figure 30: The numerical solution and the analytic solution for the last example

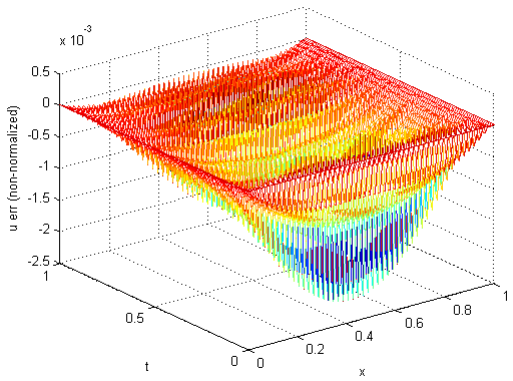

Figure 31: The absolute error between the numerical solution and the analytic solution for the last example

We also give the RMS error as a function of t for various values of grid spacing, i.e. $M = 4, 8, 16, 32, 64$ for a fixed time step $\tau = 0.01$ and the same error for a fixed $M = 16$ and various values of time steps $\tau = 0.25, 0.125, 0.0625, 0.03125, 0.015625$ in Figure 33.

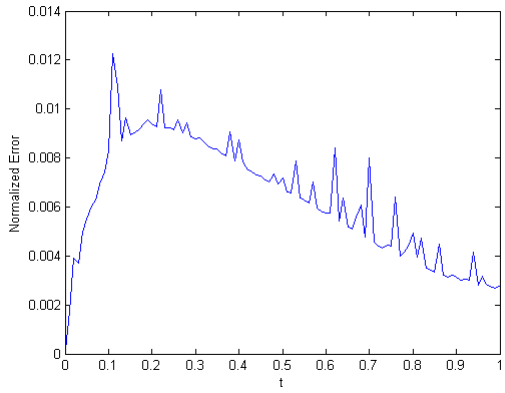

Figure 32: The RMS error as a function of t for the last example

It can be seen that the error increases initially for all M but eventually goes down, except for $M = 4$. It doesn't approach zero, since the solution grows linearly in t and quadratically in x. The error mainly decreases with increasing M. Similar situation can be seen when M is fixed and the time step is halved.

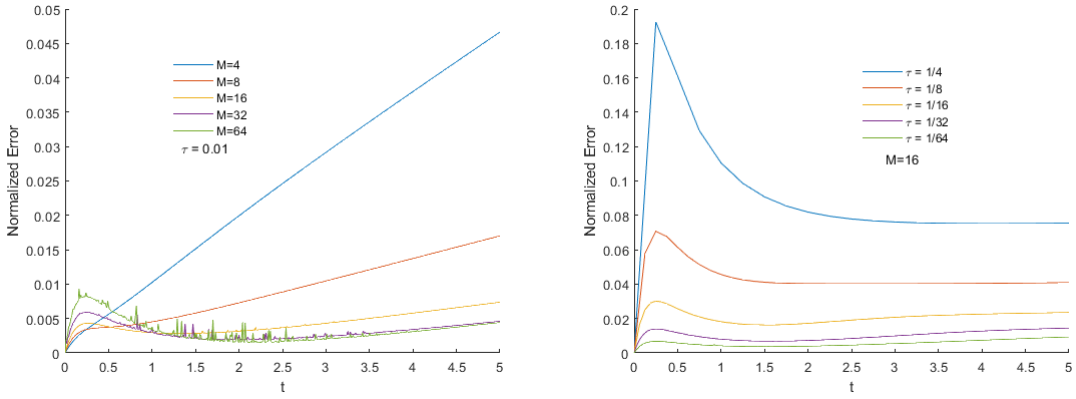

Figure 33: The RMS error as a function of t for fixed time step $\tau = 0.01$ and increasing M (left) and for fixed $M = 16$ and halving the time step for the last example

Conclusions We reported on application of the Matlab code ODE45 in the use of solving a nonlinear diffusion model with memory. Eight examples were given, demonstrating the capability of the code to solve both the cases of homogeneous and inhomogeneous boundary conditions. The generalization to a system of such equations is trivial and was discussed in the literature. Although there the authors did not use ODE45.

References

[1] T. A. Jangveladze, Z. Kiguradze, B. Neta, Numerical Solutions of Three Classes of Nonlinear Parabolic Integro-Differential Equations, Elsevier, 2016.

[2] L. Landau, E. Lifschitz, Electrodynamics of Continuous Media. Course of Theoretical Physics, Vol. 8. (Translated from the Russian) Pergamon Press, Oxford-London-New York-Paris; Addision-Wesley Publishing Co., Inc., Reading, Mass., 1960; Russian original: Gosudarstv. Izdat. Tehn-Teor. Lit., Moscow, 1957.

[3] D. Gordeziani, T. Dzhangveladze(Jangveladze), T. Korshia, Existence and uniqueness of the solution of a class of nonlinear parabolic problems, *Differ. Uravn.*, **19**, (1983), 1197–1207 (Russian). English translation: *Diff. Eq.*, **19**, (1983), 887–895.

[4] T. Dzhangveladze(Jangveladze), The first boundary value problem for a nonlinear equation of parabolic type, *Dokl. Akad. Nauk SSSR*, **269**, (1983), 839–842 (Russian). English translation: *Soviet Phys. Dokl.*, **28**, (1983), 323–324.

[5] G. Laptev, Quasilinear parabolic equations which contains in coefficients Volterra's operator, *Math. Sbornik*, **136**, (1988), 530–545 (Russian). English translation: *Sbornik Math.*, **64**, (1989), 527–542.

[6] G. Laptev, Quasilinear Evolution Partial Differential Equations with Operator Coefficients, Doctoral Dissertation, Moscow, 1990, (Russian).

[7] N. Long, A. Dinh, Nonlinear parabolic problem associated with the penetration of a magnetic field into a substance, *Math. Mech. Appl. Sci.*, **16**, (1993), 281–295.

[8] T. A. Jangveladze, On one class of nonlinear integro-differential equations, *Semin. I. Vekua Inst. Appl. Math.*, **23**, (1997), 51–87.

[9] M. Vishik, Solvability of boundary-value problems for quasi-linear parabolic equations of higher orders, (Russian). *Math. Sb. (N.S.)*, **59(101)**, (1962), suppl. 289–325.

[10] J. Lions, Quelques Méthodes de Résolution des Problèmes aux Limites Non-linéaires, Dunod, Gauthier-Villars. Paris, 1969.

[11] T. Jangveladze(Dzhangveladze), Z. Kiguradze, Asymptotics of a solution of a nonlinear system of diffusion of a magnetic field into a substance, *Sibirsk. Mat. Zh.*, **47**, (2006), 1058-1070 (Russian). English translation: *Siberian Math. J.*, **47**, (2006), 867–878.

[12] T. Jangveladze, Z. Kiguradze, B. Neta, Large time behavior of solutions to a nonlinear integro-differential system, *J. Math. Anal. Appl.*, (2008), (doi:10.1016/j.jmaa.2008.10.016, in press).

[13] T. A. Jangveladze, Convergence of a difference scheme for a nonlinear integro-differential equation, *Proc. I. Vekua Inst. Appl. Math.*, **48**, (1998), 38–43.

[14] Z. V. Kiguradze, Finite difference scheme for a nonlinear integro-differential system, *Proc. I. Vekua Inst. Appl. Math.*, **50-51**, (2000-2001), 65–72.

[15] B. Neta, J. O. Igwe, Finite differences versus finite elements for solving nonlinear integro-differential equations, *J. Math. Anal. Appl.*, **112**, (1985), 607–618.

[16] T. A. Jangveladze, Z. V. Kiguradze, B. Neta, Large time behavior of solutions and finite difference scheme to a nonlinear integro-differential equation, *Comput. Math. Applic.*, **57**, (2009), 799-811.

[17] C. Dafermos, L. Hsiao, Adiabatic shearing of incompressible fluids with temperature-dependent viscosity, *Quart. J. Appl. Math.*, **41**, (1983), 45–58.

[18] J. C. Butcher, The Numerical Analysis of Ordinary Differential Equations, Runge-Kutta and General Linear Methods, John Wiley & Sons, 1987.